A study on preparation and characterization of carbon doped TiO$_2$ nanotubes

Srimala Sreekantan[1]*, Roshasnorlyza Hazan[1], Zainovia Lockman[1] and Ishak Mat[2]

[1] School of Materials and Mineral Resources Engineering, Universiti Sains Malaysia, 14300, Nibong Tebal, Pulau Pinang, Malaysia
[2] Advance Medical and Dental Institute, Eureka Complex, Universiti Sains Malaysia, 11800, Pulau Pinang, Malaysia

ABSTRACT

The present study is directed to clarify the influence of carbon doping on the degradation of methyl orange. TiO$_2$ nanotubes were prepared by anodizing titanium foils in a two electrode configuration bath with titanium foil as the anode and platinum as the counter electrode. The electrochemical bath consists of 1 M Na$_2$SO$_4$ with 0.7 g ammonium fluoride, NH$_4$F. The nanotubes obtained were further doped with carbon via in-situ and ex-situ method. Incorporation of carbon on TiO$_2$ via in-situ method is accomplished during the anodization process by introducing oxalic acid into electrolyte while the ex-situ doping involves carbon incorporation into pre-fabricated TiO$_2$ nanotube via flame annealing using carbon blackN330. Characterization such as Scanning Electron Microscope (SEM), Energy Dispersive X-ray Analysis (EDX), and X-Ray Diffraction (XRD) are used to determine the surface morphology, composition of dopants, and phases exists. Well ordered nanotube with good adherence and smooth surface was obtained for both methods. When the oxide was annealed, X-ray diffraction analysis revealed the presence of anatase and rutile phase. The photocatalytic properties of the pure TiO$_2$ and carbon doped TiO$_2$ were tested for methyl orange degradation and the result indicated that the in-situ doped TiO$_2$ has much better degradation than the ex-situ and pure TiO$_2$. The percentage of methyl orange degradation for in-situ was 20% and 41% higher than ex-situ doped TiO$_2$ and pure TiO$_2$, respectively.

| TiO$_2$ | Nanotube | Anodization | Carbon doping | Photodegradation |

1. INTRODUCTION

Among the new materials being developed for photocatalytic activity, n-type semiconducting TiO$_2$ remains as one of the most promising materials because of its high efficiency, low cost, chemical inertness, ecofriendly nature and photostability [1,2]. Because of these great properties, TiO$_2$ would be the best candidate to be used for much application such as photocatalyst [3], impant materials [4], hydrogen sensing [5], solar cell [6] and many more. When TiO$_2$ is exposed to UV light, it could be used to convert photons into chemical or electrical energy by generating electron and holes. The electron and holes then react with surface species to produce highly oxidizing species which is capable to convert pollutants to nontoxic or less harmful substance. However, the widespread use of TiO$_2$ is hindered by its low utilization of solar energy in the visible region (about 3–5 %) because of the wide band gap. Efficient use of solar radiation requires extending the photoresponse of TiO$_2$ to visible wavelengths. Therefore, many efforts were directed towards modifying the band gap of TiO$_2$ and thus extending its photoresponse into the visible region by doping process [7-19]. Various transition metal cationic dopants have been studied [7-9] but it has been found to inhibit the photocatalytic activity of TiO$_2$.

This is because the doped TiO$_2$ suffers from a thermal instability or an increase in the recombination centres of the charge carriers [10]. Therefore, many have suggested that smaller band gap might also be achieved by incorporating anionic dopants such as nitrogen [11-14], carbon [15 -17] and sulphur [18-20] for the extension of photocataytic activity into visible region. In particular, carbon-doped TiO$_2$ was indicated as one of the best in terms of band gap narrowing. It is therefore our intention to study on band gap engineering of TiO$_2$ by carbon doping. In our previous study, we observed that few parameters affect the production of TiO$_2$ nanotubes [21-25].

Herein we report on two different methods for preparing the doped TiO$_2$. The first one involves in-situ method whereby the carbon incorporation into titanium foil was accomplished while fabricating TiO$_2$ nanotube whereas the second one is ex-situ doping which involves carbon incorporation directly on pre-fabricated TiO$_2$ nanotubes. Both methods were done via anodization. The source of dopant was oxalic acid (C$_2$H$_2$O$_4$) for in-situ method and carbon black N330 for ex-situ method.

2. EXPERIMENTAL

Anodization was done in a standard two-electrode bath with titanium as the working electrode and platinum as the counter electrode. High purity titanium foils (99.6 % purity)

Corresponding author at: School of Materials and Mineral Resources Engineering Universiti Sains Malaysia, 14300, Nibong Tebal, Pulau Pinang, Malaysia
E-mail addresses: srimala@eng.usm.my (Srimala Sreekantan)

of thickness 0.2 mm that was used in this study were purchased from STREM Chemicals. Prior to anodization, Ti foils were degreased by sonicating in acetone for 15 minutes followed by rinsing in deionised water and then dried in nitrogen stream. After drying, the foil was cut into 1 cm x 4 cm area and exposed to the electrolyte which consisted of 100 ml 1 M Na_2SO_4 with 0.7 g NH_4F. The pH of the electrolyte was measured using a digital pH meter. H_2SO_4 was added to the solution to adjust the pH. The electrochemical treatment consisted of a potential ramp from open-circuit to a fixed value of 20 V. The sweep rate was kept constant at 1 V/min. The bath was kept at room temperature. For purposes of in-situ carbon doping, oxalic acid ($C_2H_2O_4$) was included in the anodization bath for 30 minutes. After the anodization was completed, the carbon doped TiO_2 sample was annealed at 500 ^oC for 2 hours in an air atmosphere furnace. The condition is chosen based on our preliminary studies which indicate that increasing the annealing temperature to 300 ^oC shows the existence of vaguely anatase peak and for 500 ^oC induce the formation of anatase and rutile with better crystallinity [21,26]. It is anticipated that the formation of crystalline phase in carbon doped sample will lead to enhanced photodegradation activity.

As for ex-situ doping, prior to carbon incorporation, TiO_2 nanotubes were fabricated via anodization in Na_2SO_4 with 0.7 g NH_4F at pH of 4 for 30 minutes. The doping were done via flame annealing in a typical horizontal furnace with heating and cooling rates of 10 ^oC/min and the source of dopant being used is carbon black N330. Flame annealing with carbon black were done at 500 ^oC for 2 hours in saturated argon gas.

The morphologies of the anodized titanium were characterized using a Field Emission Scanning Electron Microscope (FESEM SUPRA 35VP ZEISS) operating at working distances down to 1 mm and extended accelerating voltage range from 30 kV down to 100 V. The FESEM SUPRA 35VP ZEISS was capable of energy dispersive X-ray spectroscopy (EDX). The crystal phases of the TiO_2 nanotubes were studied by X-ray diffraction using the Bruker D8 powder diffractometer operating in the reflection mode with Cu Kα radiation (40 KV, 30 mA) diffracted beam monochromator, using a step scan mode with the step size of 0.1 $^\circ$ in the range of 25-70 $^\circ$. The step time was of 3 s, adequate to obtain a good signal-to-noise ratio in the main reflections of the TiO_2 nanotube, (1 0 1) anatase (2θ = 25.3 $^\circ$) and (1 0 1) rutile (2θ = 36.1 $^\circ$). The weight fractions of the anatase and rutile phases of nanotube subjected to various heat treatment were estimated from the relative intensities of the strongest peaks corresponding to anatase and rutile respective integrated XRD peak intensities using the equation (1) [27]:

$$X_A = \left(1 + 1.26 \frac{I_R}{I_A}\right)^{-1} \tag{1}$$

where X_a is a weight fraction of anatase in powder, and I_A and I_R are the X-ray integrated intensities of the (1 0 1) reflection of anatase and (1 0 1) reflection of rutile, respectively.

The photocatalytic degradation studies was performed by dipping 7 pieces of 1 cm^2 foils made up of carbon doped TiO_2 nanotubes in 200 ml of 50 ppm methyl orange in self-constructed photoreactor which consist of a quartz glass. The sample was then left in the reactor for about 30 min in dark environment to achieve the adsorption / desorption equilibrium. It was then photoirradiated at room temperature by using TUV 18 W UV-C Germicidal light. 5 ml solution was withdrawn for every 1 hour from the quartz tube to monitor the degradation of methyle orange after irradiation. The concentration of the degradated methyl orange was determined using UV-Vis spectrometer.

3.   RESULTS & DISCUSSION

3.1   Effect of different pH on TiO_2 nanotube formation

For this set of experiment, 0.7 g of NH_4F in 100 ml, 1 M Na_2SO_4 was used for anodization but the pH of the solution was altered from 3, 4, and 5 using H_2SO_4. The bulk electrolyte without the addition of H_2SO_4 has a pH of around 6. For all experiments, anodization was conducted at 20 V for 30 minutes. Different pH of the electrolyte leads to different surface structure of TiO_2. Representative cross sections of the TiO_2 formed at different pH's are shown in Figure 1. For pH 3, the sample seemed to be inadequate for formation of TiO_2 oxide layer (Figure 1a). In some portion of the foil, a flake structure is observed and it was further confirmed with EDX. EDX analysis (the insert in Figure 1a) confirmed the absence of TiO_2 oxide layer in both area A and B. The Ti foil probably was severely etched, revealing the grain of the Ti.

Surface morphology of the TiO_2 formed at pH 4 and 5 are shown in Figure 1b and 1c. It clearly indicates that pH plays an important role for the formation of the nanotubes. It is also seen that the diameter of the tubes depends on the pH of the bath. For higher pH, e.g. pH = 4 (Figure 1b), the average diameter of the tubes was approximately 80 nm. When the pH of the bath was further increased to 5, the diameter of the tubes was smaller i.e. $\sim$ 70 nm (Figure 1c). Further observation indicates that the thickness of the prepared nanotube influenced by pH of the bath. Higher pH, i.e. pH 5 leads to the formation thicker wall approximately 15 nm while lower pH 4 results in thinner wall around 8 nm. The electrolyte pH may adjust TiO_2 dissolution rate at the pore bottom by localized acidification has been reported by Macak and co-worker [28]. Effects of migration and diffusion generate lower pH value at the pore bottom while higher pH value is obtained at the pore mouth. The smaller diameter and thicker wall of the nanotube with increasing pH is probably associated with chemical dissolubility of the electrolyte. At high pH, the formation of $[TiF_6]^{2-}$ complex is reduced and relatively result in weak chemical dissolubility.

As a result, the diameter of the tube is small and the wall thickness is wide.
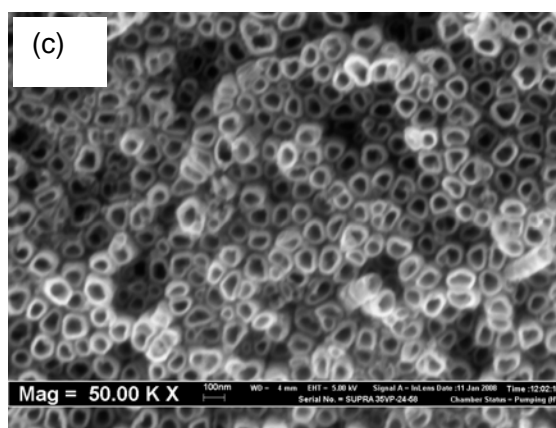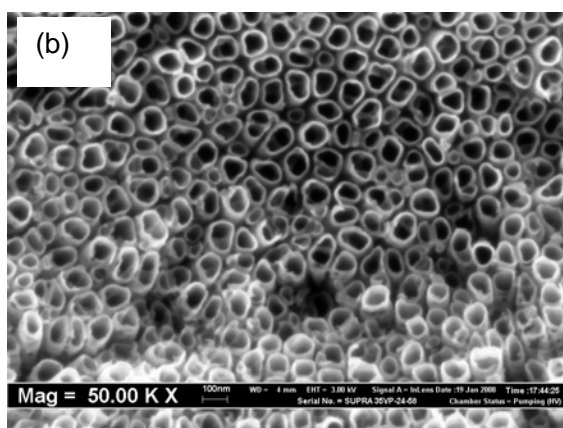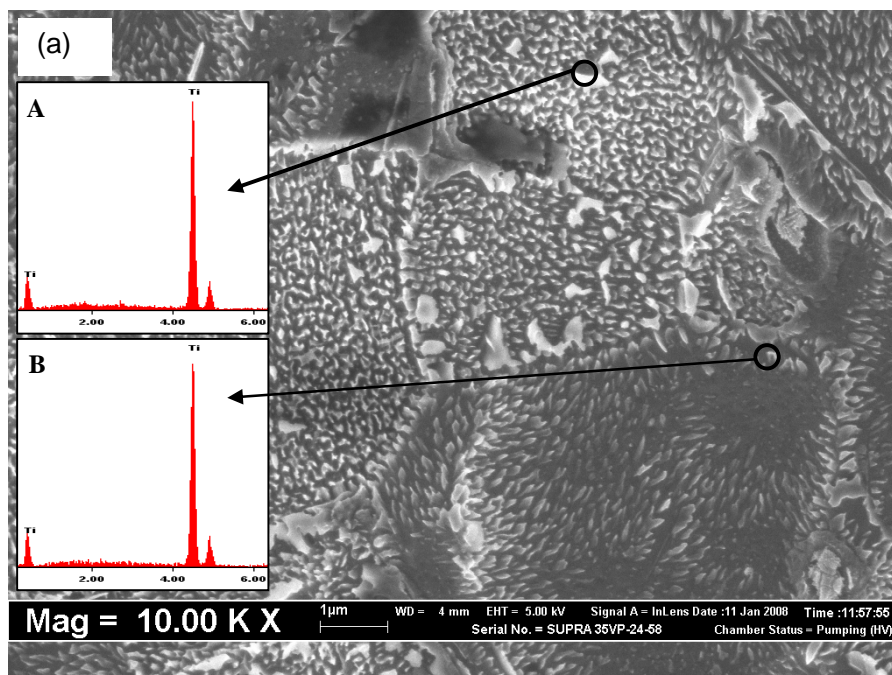
Figure 1: FESEM images of the TiO$_2$ nanotubes obtained with different pH (a) pH 3, (b) pH 4 and (c) pH 5

3.2 Formation of carbon doped TiO$_2$ nanotube via in-situ and ex-situ method

From the first part of experiment, production of TiO$_2$ nanotubes were found to be very well defined over the whole area of the foil (not shown) when the pH of the bath is 4. Therefore, for the next set of experiment, the pH of the solution was fixed to 4. Figure 2, shows FESEM image of a carbon doped TiO$_2$ nanotubes with insets showing the length of the tubes. The tubes were obtained by in-situ doping technique using oxalic acid as a carbon source in 1 M Na$_2$SO$_4$ at room temperature for 30 minutes. TiO$_2$ nanotubes with diameter of 80 nm and length of 1.3 μm are obtained. The wall thickness was approximately 20 nm.

EDX analysis was performed to clarify the incorporation of carbon on the prepared tubes. Representative EDX spectrum of the in-situ carbon doped TiO$_2$ is shown in Figure 3. Twenty measurements were performed on each sample and average values were taken. The data demonstrate that the amount of doped carbon into TiO$_2$ tubes was in the range of 6.3-6.5 %, hence indicating that the tubes possess uniform carbon content when anodized for 30 minutes. After the anodization was completed, the in-situ carbon doped TiO$_2$ sample was annealed at 500 °C for 2 hours in an air atmosphere furnace. The morphology of the tubes after heat treatment was analyzed by FESEM and the result indicates no variation in the structure of the oxide

(not shown) as compared to the structure formed before subjected to annealing process.

Figure 4 shows an illustrative FESEM image of TiO_2 nanotube that have been doped with carbon black N330 via ex-situ method using flame annealing technique. Under this condition, the nanotubes have a length of 1.2 μm with wall thickness of 20 nm. The average nanotube diameter as calculated from the FESEM image was 80 nm, similar to in-situ doped sample. Representative EDX spectrum of the ex-situ doped TiO_2 is shown in Figure 5 and it was found that the average carbon content of the ex-situ doped TiO_2 was slightly lower (5.14 %) as compared to in-situ doped TiO_2. This is probably attributed to easier diffusion of oxalic acid due to its smaller size compared to carbon black.

3.3   XRD analysis

Figure 6 shows the crystal structure of pure TiO_2 and carbon doped TiO_2 nanotube which was produced after flame annealing. The result clearly shows the crystal structure of TiO_2 depends on the annealing treatment. XRD of the as-anodized sample (without dopant and annealing process) in Figure 6a indicated that the self-organized TiO_2 nanotubes have amorphous structure as only Ti-peaks were shown. Habazaki has reported the formation of crystalline oxide in a film formed at 20 V [29]. In contrast to their finding, amorphous phase has been observed in this study and probably it is associated with the formation of localized crystalline oxides and not a continuous one throughout the oxide. However if the same sample heated at 500 °C, it matches the reference pattern (ICDD card number 21-1272) of anatase at 2θ = 25.28 °, 48.05 °, 53.89 °, 55.06 ° and 62.69 ° and rutile phase (ICDD card number 21-1274) at 36.08 °, 41.23 ° and 54.32 °, indicating transformation form amorphous structure to crystalline structure (Figure 6b). The weight fractions of the anatase and rutile phase were approximately 50.2 % and 49.8 %, respectively. Similar phase structure was also found in in-situ carbon doped nanotube (Figure 6c) with 62.8 % of anatase and 37.2 % rutile phases.
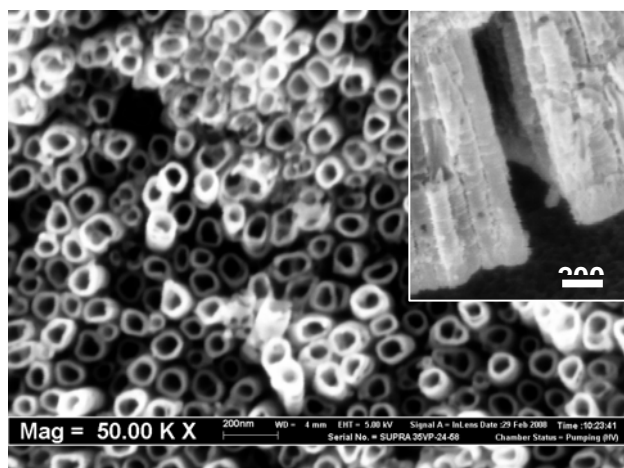
**Figure 2**: FESEM images of the carbon doped TiO_2 nanotubes obtained via in-situ method
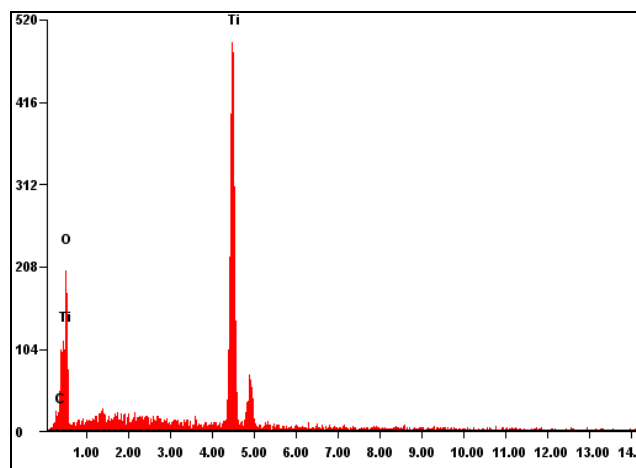
Figure 3: EDX spectrum of the carbon doped TiO_2 nanotubes obtained via in-situ method
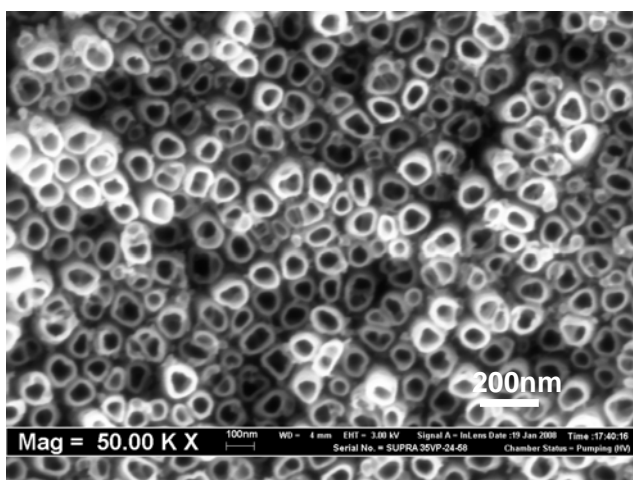
Figure 4: FESEM images of the carbon doped TiO_2 nanotubes obtained via ex-situ method
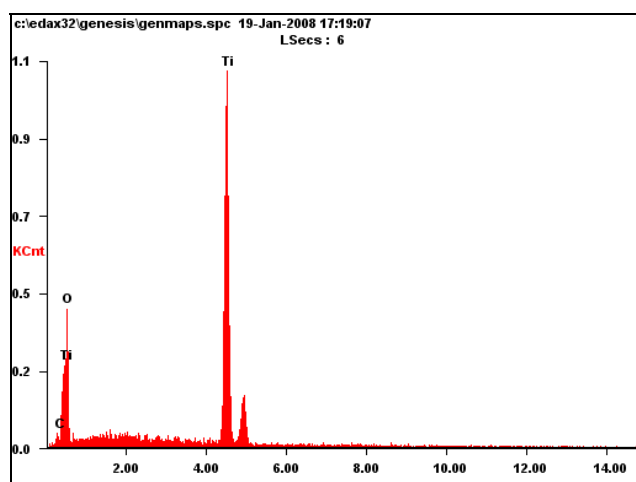
Figure 5: EDX spectrum of the carbon doped TiO_2 nanotubes obtained via ex-situ method
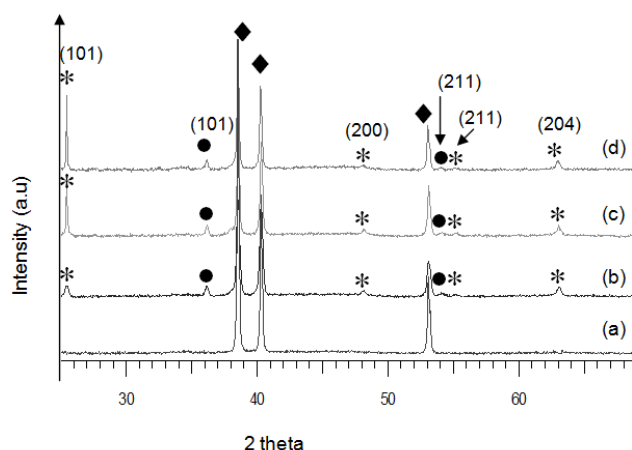
Figure 6: XRD pattern of (a) pure TiO$_2$ and not annealed (b) pure TiO$_2$ and annealed (c) in-situ carbon doped and annealed (d) ex-situ carbon doped and annealed [♦:Ti, ●: rutile, ∗: anatase]

Figure 6d shows the XRD pattern of the ex-situ doped TiO$_2$ after flame annealed for 2 hours in carbon black. In addition to the observed prominent Ti peak, there are small peak at 2θ values of 25.28 $^\circ$, 48.05 $^\circ$, 53.89 $^\circ$, 55.06 $^\circ$ corresponding to the anatase phase (ICDD card number 21-1272) and at 2θ values of 36.08 $^\circ$, 41.23 $^\circ$ and 54.32 $^\circ$ corresponding to rutile (ICDD card number 21-1274) TiO$_2$. The weight fractions of the anatase and rutile phases of doped nanotube were 66.7 % and 33.3 %, respectively. It is worth to note that the weight fraction of anatase in carbon doped sample via in-situ and ex-situ is higher by 12 % and 16 % respectively as compared to the pure sample. The precious reason for the higher fraction of anatase in carbon doped sample are currently unclear and the subject of ongoing studies. However, based on our preliminary studies it is possible that oxygen rich atmospheric condition be an important factor in the formation of rutile phase (Table 1).

Table 1: Anatase to rutile ratio and the oxygen content during the annealing process for doped and undoped TiO$_2$

Samples	Undoped TiO$_2$ after annealing	In-situ Carbon doped	Ex-situ Carbon doped
XRD Analysis	Anatase and Rutile	Anatase and Rutile	Anatase and Rutile
Ratio of anatase: rutile	50.2 : 49.8	62.8 : 37.2	66.7 : 33.3
Atmospheric condition during annealing process	Oxygen content are relatively high as compared to insitu and exsitu doped TiO$_2$ because flame annealing was done in air	Probably carbon incoparation during anodization have influence on the atmospheric condition during annealing process. Therefore oxygen content is lower as compared to pure TiO$_2$	Oxygen content are the lowest because flame annealing with carbon black were done in saturated argon gas

3.4 Photocatalytic activity

The photocatalytic activity of the pure TiO$_2$ and doped (in-situ and ex-situ) TiO$_2$ nanotube was evaluated by photodegrdation of methyl orange aqueous solution. Figure7a and 7b show the changes in absorption spectra of the methyl orange aqueous solution during its photodegradation using in-situ and ex-situ doped TiO$_2$ nanotube, respectively. It could be seen the absorption peak gradually decreased with increasing UV irradiation time and this is attributed to the generation of electron and holes which is increasing with the irradiation time. After UV irradiation for 5 hours, the absorption peak of methyl orange aqueous solution for doped sample was weak. For comparison, the absorption spectrum of the pure TiO$_2$ was also measured after 5 hours and it is shown in Figure 7c. The experimental observation indicated that the colour of the methyl orange aqueous solution changed from dark orange to a pale orange or colourless one, depending on the pure TiO$_2$ or doped TiO$_2$. The colour changes actually indicating the degradation of methyl orange. To quantify the observed trends in Figure 8, the absorbance was converted to concentration with the following equation ;

$$\ln\left(\frac{C_o}{C_t}\right) = \ln\left(\frac{A_o}{A_t}\right) = kt \qquad (2)$$

Here C_o is the initial dye concentration (at the end of sorption period), while C_t is the actual dye concentration. A_o is the initial absorption value while A_t is the actual absorption value, k is rate constant, t is the time after UV irradiation.

Figure 8 shows the plots of methyl orange concentration versus irradiation time for in-situ and ex-situ doped sample. Illumination in the absence of photocatalyst did not result in the photodegradation (not shown). It was found that the in-situ doped TiO_2 showed the greatest degradation whereby the concentration of methyl orange decreased rapidly by 69 % after UV irradiation for 5 hours. As for ex-situ doped TiO_2 nanotubes, the concentration decrease by 49 %. Pure TiO_2 showed the lowest photodegradation whereby the concentration of methyl orange decreased by 28 %. Based on the results obtained, it seems that crystal structure is one of the important factors

affecting the photocatalytic activity. According to Bakardjieva [17], TiO_2 nanotubes with 70 % anatase and 30 % rutile are the optimum ratio and showing great efficiency for photocatalytic activity. The similar observation can be seen in this work. In-situ and ex-situ carbon doped TiO_2 with 62 % and 66 % of anatase, respectively showed better performance in the photodegradation of methyl orange as compared to pure TiO_2 with 50 % anatase. Less activity of pure TiO_2 might be due to lack of anatase phase which can assist to reduce the rapid rate of recombination in rutile phase. Besides, pure TiO_2 has no absorption above 400 nm. However, the carbon doped TiO_2 results in obvious absorption up to 700 nm [30]. This absorption features suggest that carbon doped TiO_2 can be activated by visible light to enhance the electron transfer and thus improve the photodegradation of methyl orange.
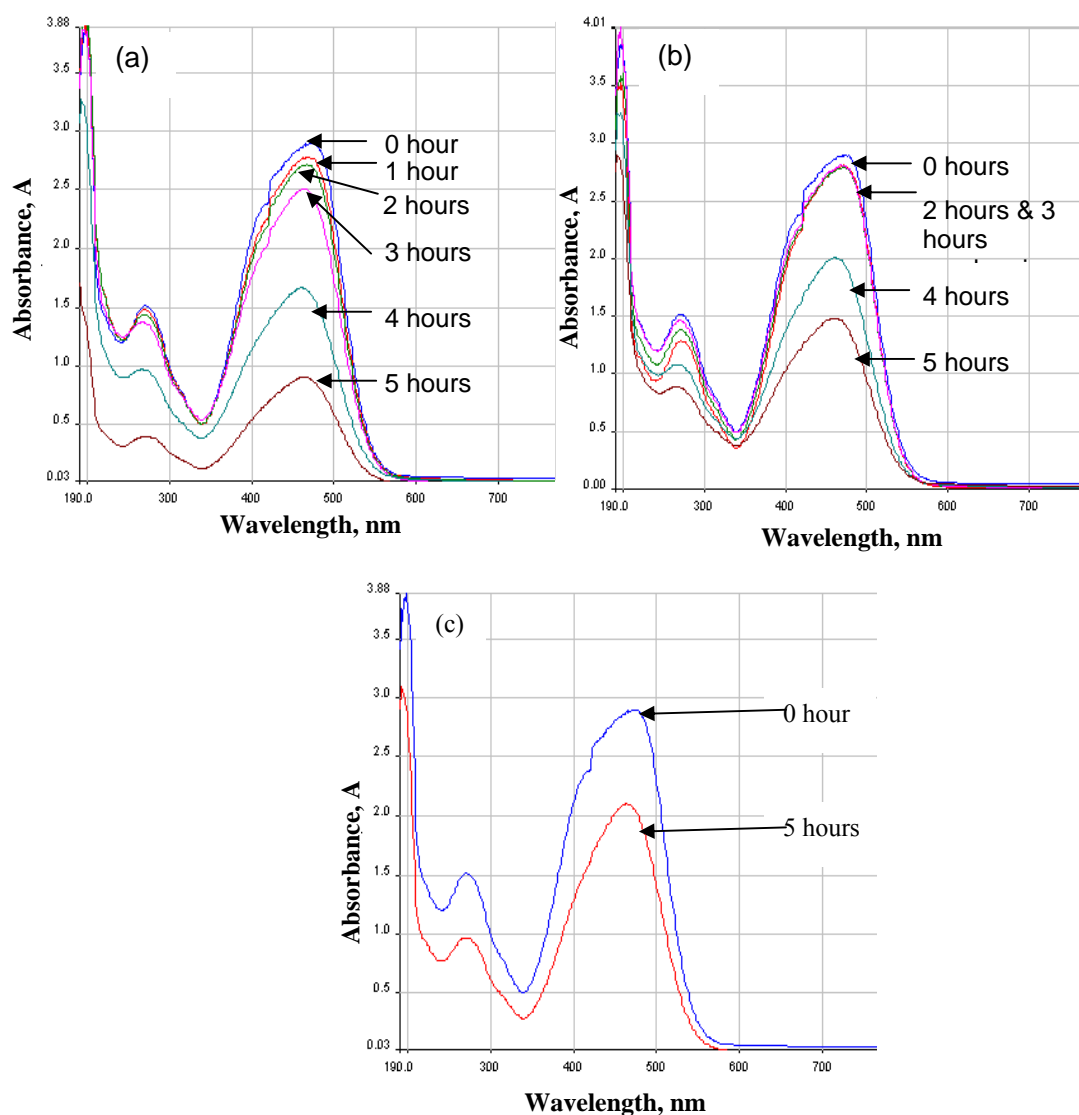

Figure 7: Analysis of absorbance of methylene orange undergo photocatalytic testing with (a) in-situ carbon doped TiO_2 (b) ex-situ carbon doped TiO_2 and (c) pure TiO_2
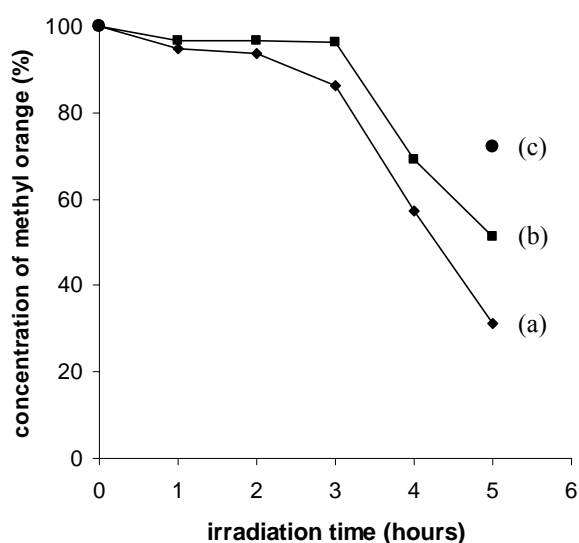
Figure 8: Plots of methyl orange concentration versus irradiation time for
(a) in-situ, (b) ex-situ doped sample and (c) pure TiO_2

4.   CONCLUSION

In summary, anodization of the Ti foil at pH 4 resulted in a well organized TiO_2 nanotube. Approximately 6.4 % and 5.1 % carbon was incorporated into TiO_2 by in-situ and ex-situ method, respectively. This result indicates in-situ method is more efficient than ex-situ method to prepare carbon doped TiO_2. XRD pattern of the sample annealed at 500 ^{o}C indicated the presence of crystalline anatase and rutile phase. It appears that crystal structure and carbon content are an important factor affecting the photocatalytic activity. In this work, it was found in-situ doped TiO_2 with 62 % of anatase and 38 % rutile had degraded the methyl orange by 69 %, which is 20 % and 41 % higher than ex-situ and pure TiO_2, respectively.

REFERENCES

[1]   M.R. Hoffmann, S.T. Martin, W. Choi, D.W. Bahnemann, Chem. Rev. 95 (1995) 69–96.
[2]   A. Fujishima, K. Hashimoto, T. Watanabe, BKC Inc., Tokyo, 1999.
[3]   Z. Liu, X. Zhang, S. Nishimoto, T. Mukarami, A. Fujishima, Environ. Sci. Technol. 42 (2008) 8547-8551.
[4]   V. S. Saji, H. C. Choe, W. A. Brantley, Acta Biomaterialia, 5 (2009) 2303-2310.
[5]   G. K. Mor, M. A. Carvalho, O. K. Varghese, M. V. Pishko, C. A. Grimes, J. Mater. Res, 19 (2004) 628-634.
[6]   K. Zhu, T. B, Vinzant, N. R. Neale, A. J. Frank, Nano Letters, 7 (2007) 3739-3746.
[7]   K.E. Karakitsou, X.E. Verykios, J. Phys. Chem. 97 (1993) 1184–1189.
[8]   W. Choi, A. Termin, M.R. Hoffmann, J. Phys. Chem. 98 (1994) 13669–13679.
[9]   H. Yamashita, M. Harada, J. Misaka, M. Takeushi, M. Anpo, J. Photochem. Photobiol. A 148 (2002) 257–261.
[10]   Wang H., Lewis J.P., Journal of physics: Condense Matter Vol. 18 (2006) 421-434.
[11]   T. Morikawa, R. Asahi, T. Ohwaki, K. Aoki, Y. Taga, Jpn. J. Appl. Phys., Part 2 40 (2001) L561–L563.
[12]   Y. Aita, M. Komatsu, S. Yin, T. Sato, J. Solid State Chem. 177 (2004) 3235–3238.
[13]   R. Asahi, T. Morikawa, T. Ohwaki, K. Aoki, Y. Taga, Science 293 (2001) 269–271.
[14]   Y.Wang, C.X. Feng, Z.S. Jin, J.W. Zhang, H.J. Yang, S.L. Zhang, J.Mol. Catal. A: Chem. 260 (2006) 1–3.
[15]   S. Sakthivel, H. Kisch, Angew. Chem. Int. Ed. 42 (2003) 4908–4911.
[16]   C.S.Kuo,Y.H. Tseng, C.H. Huang,Y.Y. Li, J. Mol. Catal. A: Chem. 270 (2007) 93–100.
[17]   J. Lin, R. Zong, M. Zhou, Y. Zhu, Appl. Catal. B: Environ., 89 (2009) 425-431.
[18]   T. Umebayashi, T. Yamaki, H. Ito, K. Asahi, Appl. Phys. Lett. 81 (2002) 454–456.
[19]   T. Ohno, T. Mitsui, M. Matsumura, Chem. Lett. 32 (2003) 364–365.
[20]   J.C. Yu, W.K. Ho, J.G. Yu, H. Yip, P.K.Wong, J.C. Zhao, Environ. Sci. Technol. 39 (2005) 1175–1179.
[21]   S. Sreekantan, R. Hazan, Z. Lockman, Thin Solid Film 518 (2009) 16-21
[22]   S. Sreekantan, Z. Lockman, R. Hazan, M. Tasbihi, L. K. Tong, A. R. Mohamed, Journal of Alloys and Compounds 485 (2009)478-483
[23]   S. Sreekantan, R. Hazan, K. A. Saharudin, I. Mat. MicroSoM (Buletin of the Electron Microscopy Society of Malaysia), 7 (2009) 7-9.
[24]   R. Hazan, S. Sreekantan, A. Abdul Khalil, I. M. S. Nordin, I. Mat., Journal of Physical Science, 20 (2009) 35-47.
[25]   S. Sreekantan, R. Hazan, Z. Lockman, Synthesis, Solid State Science and Technology, 17 (2009) 132-139.

[26] N. A. Jani, Z.Lockman, S. Sreekantan, L. Schmidt-Mande, J. Driscoll , International Conference on X-Rays and related Technique in Research and Industries (2008), 58

[27] S. Bakardjieva, J. Subrt, V. Stengl, M. J. Dianez, M. J. Sayagues, Applied Catalysis B: Environmental 58 (2005) 193–202

[28] J. M. Macak, H. Tsuchiya, L. Taveira, S. Aldabergerova, P. Schmuki, Angew. Chem. Int. Ed., 44 (2005) 7463-7465.

[29] H.Habazaki, M.Uozomi, H.Konno, K.shimizu, P.Skeldon, G.E.Thompson, Corrosion Science, vol. 45, pp. (2003)2063-2073

[30] Y.Li, D.S.Hwang, N.H. Lee, S.J.Kim. Chemical Physics Letters 404 (2005) 25-29